Comparative study on dry etching of alpha- and beta-SiC nano-pillars

J H Choi, L Latu-Romain, E Bano, Anne Henry, W J Lee, T Chevolleau and T Baron

Original Publication:

J H Choi, L Latu-Romain, E Bano, Anne Henry, W J Lee, T Chevolleau and T Baron, Comparative study on dry etching of alpha- and beta-SiC nano-pillars, 2012, Materials letters (General ed.), (87), , 9-12.
http://dx.doi.org/10.1016/j.matlet.2012.07.051

Comparative study on dry etching of α- and β-SiC nano-pillars

J. H. Choi[a,b,*] , L. Latu-Romain[b], E. Bano[a], A. Henry[c], W. J. Lee[d], T. Chevolleau[b], and T. Baron[b]

[a] IMEP-LAHC, Grenoble INP - MINATEC, 3 Parvis Louis Néel, BP257, 38016 Grenoble Cedex 1, France
[b] LTM/CNRS, 17 rue des Martyrs (CEA-LETI), 38054 Grenoble Cedex 9, France
[c] Department of Physics, Chemistry and Biology, Linköping University, SE-581 83 Linköping, Sweden
[d] Electronic Ceramics Center, Department of Nano Technology, Dong-Eui University, Busan 614-714, Korea

Abstract

Different polytypes (α-SiC and β-SiC) and crystallographic orientations ((0001) and (11-20) of 6H-SiC) have been used in order to elaborate Silicon Carbide (SiC) nanopillars using inductively coupled plasma etching method. The cross section of the SiC pillars shows a rhombus, pentagon, or hexagonal morphology depending on polytypes and crystallographic orientations. The favored morphologies of SiC nanopillars are originated from a complex interplay between their polytypes and crystal orientations, which reflects the so-called Wulff's rule.

Keywords: Nanopillars, Dry etching, Silicon carbide, polytypes

1. Introduction

One-dimensional (1D) SiC materials, in particular nanowires (NWs), have recently attracted much attention due to their unique physical and chemical properties, coupled with the advantages of an 1D structure. Many efforts have been carried out to fabricate the SiC nanostructures by the bottom-up methods, such as vapor-liquid-solid [1] or vapor-solid method [2]. However, those as-grown SiC NWs significantly suffer from a high density of structural defects, such as stacking faults, and unintentional high n-type doping level (~ 10^{19} – 10^{20}

* Corresponding author. Tel.: +33 4 56 52 94 77; Fax: +33 4 56 52 95 01.
E-mail address: choiji@minatec.grenoble-inp.fr

cm^{-3}). These characteristics of as-grown SiC NWs lead to poor electrical performance (such as weak gate effect and low mobility) of the related devices [3]. Therefore, top down approach is consider as a possible solution to achieve high crystalline SiC nanostructures with less structural defects and controlled doping level. Inductively coupled plasma (ICP) etching is widely used for top-down processing of SiC due to highly anisotropic profile, high etch rate, and less etch damage compared with other dry etching methods [4, 5]. Up to now only few studies on ICP etching on single crystalline SiC substrate have been reported for the fabrication of the SiC nanostructures [6, 7] . In our previous etching study using 4H-SiC (0001) substrate [7], the etching profile evolution from a circular to a hexagonal pillar shape has been observed with increasing of the etching time, which originated from the crystallographic structure of the α-SiC. However, there is still a lack of understanding of the etch behavior, such a dependence of polytypes and crystal orientations.

An interesting properties of SiC is that different polytypes (such as, α- and β-SiC) of SiC have different physical properties, that originate from the different stacking sequences of the Si-C layers. If a top-down approach is applied into these different polytypes of SiC layer, the SiC nanostructures may easily be achieved with different physical properties, which can lead to further exploit the applications of SiC nanostructures. In this letter, the etching behavior of SiC nanopillars depending on the different polytypes and crystallographic orientations: 4H-SiC (0001), 6H-SiC (0001), 6H-SiC (11-20) and 3C-SiC (001), is presented.

2. Experimental details

Experiments in SF_6/O_2 based plasma are carried out in a commercial high-density plasma etching chamber from Applied Materials Inc. [8]. The α-SiC substrates used in this study were product grades of Tankeblue 4H and 6H-SiC (0001) on-axis substrates [9]. The 6H-SiC (11-20) substrates were grown by the conventional physical vapor transport method, which has been presented elsewhere [10]. For β-SiC (001) substrate, the 3C-SiC layers were heteroepitaxially grown on Si (001) substrates [11]. For the etch masks, circular patterns with 300 ± 10 nm diameter are patterned with the same pitch distance (5 μm) on the Si face of the SiC substrate using electron beam lithography (JSM-7401F, JEOL). After developing the exposed resist, a Ni metal layer with 110 nm thickness was deposited on the Si face of the SiC substrates by e-beam evaporation. Then, liftoff process is performed at 40 °C using the remover AR 300-70. In our previous study, Ni has been evaluated as better mask material than other materials (Al and Cu) [7].

During the experiment, the following parameters: total gas flow rate, ICP coil power, substrate bias voltage and chamber pressure remain constant at 50 sccm (SF_6= 40 sccm and O_2= 10 sccm), 1500 W, 150 V, and 6 mTorr, respectively. The etched profiles of SiC nanostructures were characterized by scanning electron microscope (SEM).

3. Results and discussions

Figure 1 shows top-view SEM images of the etched SiC nanopillars with different polytypes and crystallographic orientations after etching during 360 sec, 700 sec and 840 sec, respectively. The mask size and thickness considerably decrease during the etching process due to strong physical sputtering of energetic ions, and it is completely removed after the etching during 840 sec. Therefore, the SiC nanopillars are no longer protected by the mask after long etching and begin to be etched. Finally, it clearly reveals their transversal cross section, perpendicular to the z-axis of the SiC pillar (see top-view images in Figure 1i-l). Consistent with the results of a previous study [7], continuous etching in SF_6/O_2 plasma on α-SiC (0001) substrates causes that the pillar starts to transform into a hexagonal symmetry (Figure 1a-b, 1e-f and 1i-j). The 6H- and 4H-SiC (0001) on-axis substrates show exactly the same etching behavior. In both cases, one edge of the hexagon is parallel to the <11-20> direction of the α-SiC.

It is interesting to note that the etched SiC nanopillars on the 3C-SiC (001) substrate gradually transform into a rhombic pyramid structure (Figure 1c, 1g and 1k). For the best of your knowledge, this shape has never been reported in the literature. The two diagonals of a rhombus are corresponding to the direction of [-110] and [110], respectively. The facet appearing on the top of 3C-SiC (001) nanopillar clearly shows a rhombus shape (Figure 1k). Generally, most as-grown SiC NWs fabricated by the bottom-up methods are cylinder shaped of β-SiC structure oriented towards the [111] direction [1, 2]. For heteroepitaxial growth of 3C-SiC on Si substrate, Si (001) plane is commonly used to minimize the density of planar defects, such as twin boundaries and anti-phase boundaries, with increasing thickness through mutual canceling [12, 13]. In addition, it is also possible to achieve thick SiC epitaxial layers on large area substrates using Si (001) substrate. In the present case, the etched pillars β-SiC exhibits a crystal orientation with [001] direction.

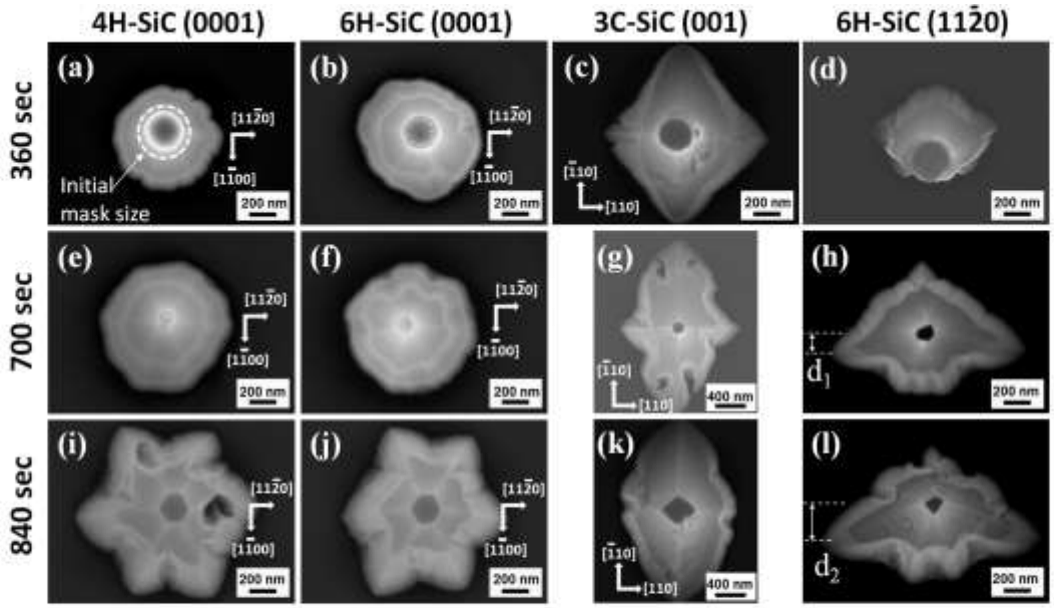

Figure 1. Top-view SEM images of SiC nanopillar after etching for (a-d) 360 sec, (e-h) 700 sec, and (i-l) 840 sec with different polytypes and crystallographic orientations. (a, e, i) 4H-SiC (0001) on-axis, (b, f, j) 6H-SiC (0001) on-axis, (c, g, k) 3C-SiC (001), and (d, h, l) misoriented 6H-SiC (11-20), respectively.

It seems that the etching behavior of SiC nanopillars is quite similar to the growth of SiC structure. The growth of 3C-SiC heteroepitaxial layer on mesa structure with different polytype substrates have gradually expanded into a hexagonal shape on 4H-SiC (0001) and a rhombus shape on Si (001) during reactions, respectively [14, 15]. These phenomena are well explained by in-plane anisotropy of the growth rate. In the same way, the sufficiently long etching process imposes developing of the planes with the lowest etch rates in all the different polytypes and crystal orientations.

The morphology of etched SiC nanopillars on 6H-SiC (11-20) substrate shows an asymmetric pillar shape at the initial stage of etching (Figure 1d and 1h), and further etching makes the pillars appear with a distorted pentagon-based pyramid structure (Figure 1l). This unique morphology of SiC pillar is related to the unintentional misorientation crystal plane toward the [0001] directions.

For the growth of 6H-SiC (11-20) substrates used in this study, α-plane seeds were prepared by attaching four equivalent rectangular samples (15 mm × 50 mm) of the α-plane in parallel and the additional process (grinding) to make a circular shape [10]. The grooves near the connected regions induce the unintentional off-axis of the (11-20) plane. Hence, the α-plane after reactions is slightly misoriented. As a result, the etched SiC pillars on 6H-SiC (11-20) substrate are tilted at an angle of misorientation, just like the leaning tower of Pisa, instead of standing upright. The apex of pillar moves from the center rhombus towards the [0001] direction (Figure 1h and 1l).

The misorientation degree (θ) of α-plane can be roughly estimated from the following formula:

$$\theta=\tan^{-1}(d/h), \qquad (1)$$

where d is the apex-shift distance and h is the pillar height.

The estimated misorientation degrees (θ) are around 1.6º and 3.0º from Figure 1h (d_1= 160 nm, h_1= 5.8 µm) and Figure 1l (d_2= 300 nm, h_2= 5.6 µm), respectively. And it ranges between 1.0º and 3.0º over the entire sample area.

Several etching techniques are used for the evaluation of the crystal quality, the determination of defect types and SiC polytypes [16, 17]. ICP dry etching of the SiC nanopillars can also be used to estimate the misorientation degree of the crystal planes. The top view of SiC pillar on 6H-SiC (11-20) substrate shows a distorted pentagonal shape due to the misorientation of α-plane, as shown in Figure 1l.

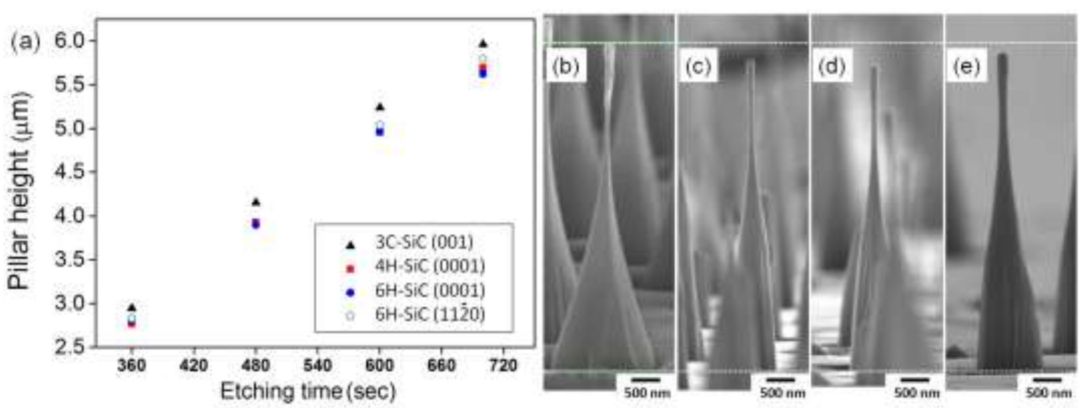

Figure 2. (a) Pillar height for different polytypes and orientations as a function of etching time, (b-e) the morphology of etched SiC pillars after 700 sec etching time, (b) 3C-SiC (001), (c) 4H-SiC (0001), (d) 6H-SiC (0001) and (e) 6H-SiC (11-20), respectively.

Figure 2a shows the SiC nanopillars height with different polytypes and crystallographic orientations as a function of the etching time. The pillar height was proportional to the etching time. The time-averaged etch rate of 3C-SiC pillar (510 nm min^{-1}) is slightly larger than that of hexagonal SiC polytypes (490 – 500 nm/min^{-1}). It is thought that low crystalline quality of heteroepitaxially grown 3C-SiC layer, which is induced by the large lattice mismatch (almost 20%) between the 3C-SiC layer and the Si substrate, could be one of the possible reasons of higher etch rates than in the case of the single crystal substrates of α-SiC [18]. The observed trend is comparable to the results reported elsewhere [19], which shows the etch-pit depth of 3C-SiC higher than that of other polytypes. In another study, the depth of etch pit decreased with increasing the hexagonality of SiC [19]. But, there is no obvious difference in etch rates of SiC pillars according to hexagonal polytypes and crystallographic orientations.

Figure 2b-e show the etching profile of SiC pillars with different polytypes and crystallographic orientations after 700 sec etching time. The minimum diameter of etched pillars on β-SiC (001) and α-SiC (0001) on-axis substrates can be shrunk into 80 nm owing to the mask erosion [7]. The length of these pillars (below 100 nm in diameter) is around 1.5 μm, which is long enough for the fabrication nano field-effect transistors (FET). The diameter of SiC pillars on 6H-SiC (11-20) substrate is slightly larger than 100 nm (around 110 nm), but it can be further decreased below 100 nm by optimizing the etching time.

In this work, large circular patterns (300 nm diameter) have been used to elaborate SiC nanopillars with a diameter less than 100 nm because the Ni mask erosion was inevitable during the etching process. However, if robust mask material (such as Al_2O_3) with small pattern size is used, longer SiC nanopillars with small diameter could be achieved without any significant pillar narrowing caused by the mask erosion [20]. The Bosh process could also be another promising method to realize straight high-aspect-ratio SiC nanopillars [21].

4. Conclusions

SiC nanopillars have been obtained using ICP etching method with different starting materials. The investigated materials were various polytypes substrates (α-SiC and β-SiC) and with different crystal orientations ((0001) and (11-20) of 6H-SiC). The morphology of etched SiC nanopillars has shown interesting features depending on the polytypes and crystal orientations. A hexagonal and rhombus based pillar structures have been obtained using α-SiC (0001) and β-SiC (001) substrates, respectively. In particular, the rhombus pyramids shape of 3C-SiC pillars is for the first time reported in the present study. The etched SiC nanopillars on 6H-SiC (11-20) show a distorted pentagon based pyramid structure due to the crystal misorientation during the growth. The misorientation angle of crystal plane 6H-SiC (11-20) can be estimated from the morphology of SiC nanopillar. Our work demonstrates the possibility to control the cross section of SiC nanopillars by selecting the polytypes and crystal orientations of substrates. This can strongly influence the emission characteristic and gate interfaces, when the SiC nanopillars are applied into practical applications, such as field emitter and nano FET.

Acknowledgments

The authors thank the staffs of the Plateforme Technologique Amont (PTA), Grenoble, France for their technical support. J. H. Choi would like to thank Jean-Luc Thomassin and Martine Gri for their assistance.

References

[1] Seong HK, Choi HJ, Lee SK, Lee JI, Choi DJ. Optical and electrical transport properties in silicon carbide nanowires. Appl Phys Lett 2004;85:1256-8.

[2] Bechelany M, Brioude A, Stadelmann P, Ferro G, Cornu D, Miele P. Very long SiC-based coaxial nanocables with tunable chemical composition. Adv Funct Mater 2007;17:3251-7.

[3] Rogdakis K, Seoung-Yong L, Bescond M, Sang-Kwon L, Bano E, Zekentes K. 3C-Silicon carbide nanowire FET: An experimental and theoretical approach. IEEET Electron Dev 2008;55:1970-6.

[4] Liudi J, Plank NOV, Blauw MA, Cheung R, van der Drift E. Dry etching of SiC in inductively coupled Cl_2/Ar plasma. J Phys D Appl Phys 2004;37:1809-14.

[5] Plank NOV, Blauw MA, van der Drift EWJM, Cheung R. The etching of silicon carbide in inductively coupled SF_6/O_2 plasma. J Phys D Appl Phys 2003;36:482-7.

[6] Kathalingam A, Kim MR, Chae YS, Sudhakar S, Mahalingam T, Rhee JK. Self assembled micro masking effect in the fabrication of SiC nanopillars by ICP-RIE dry etching. Appl Surf Sci 2011;257:3850-5.

[7] Choi JH, Latu-Romain L, Bano E, Dhalluin F, Chevolleau T, Baron T. Fabrication of SiC nanopillars by inductively coupled SF_6/O_2 plasma etching. J Phys D Appl Phys 2012;45:23520.

[8] Cunge G, Inglebert RL, Joubert O, Vallier L, Sadeghi N. Ion flux composition in HBr/Cl_2/O_2 and HBr/Cl_2/O_2/CF_4 chemistries during silicon etching in industrial high-density plasmas. J Vac Sci Technol B 2002;20:2137-48.

[9] Tankeblue, <http://www.tankeblue.com>

[10] Yeo IG, Yang WS, Park JH, Ryu HB, Lee WJ, Shin BC, Nishino S. Two-inch a-plane (11-20) 6H-SiC crystal grown by using the PVT method from a small rectangular substrate. J Korean Phys Soc 2011;58:1541-4.

[11] Henry A, Janzén E, Mastropaolo E, Cheung R. Single crystal and polycrystalline 3C-SiC for MEMS Applications. Mater Sci Forum 2009; 615-617: 625.

[12] Nagasawa H, Yagi K. 3C-SiC Single-crystal films grown on 6-inch Si substrates. Phys Status Solidi B 1997;202:335-58.

[13] Ishida Y, Takahashi T, Okumura H, Sekigawa T, Yoshida S. The APD annihilation mechanism of 3C-SiC hetero-epilayer on Si (001) substrate. Mater Sci Forum 2000;338-342:253.

[14] Lorenzzi J, Lazar M, Tournier D, Jegenyes N, Carole D, Cauwet F, Ferro G. 3C–SiC heteroepitaxial growth by vapor–liquid–solid mechanism on patterned 4H–SiC Substrate using Si–Ge melt. Cryst Growth Des 2011;11:2177-82.

[15] Nagasawa H, Yagi K, Kawahara T. 3C-SiC hetero-epitaxial growth on undulant Si (001) substrate. J Cryst Growth 2002;237–9:1244-9.

[16] Marshall RC, Faust JW. Silicon carbide. Columbia: University of South Carolina Press, 1973.

[17] Yang Y, Chen Z. Identification of SiC polytypes by etched Si-face morphology. Mat Sci Semicon Proc 2009;12:113-7.

[18] Padiyath R, Wright RL, Chaudhry MI, Babua SV. Reactive ion etching of monocrystalline, polycrystalline, and amorphous silicon carbide in CF_4/O_2 mixtures. Appl Phys Lett 1991;58:1053.

[19] Hatayama T, Koketsu H, Yano H, Fuyuki T. Hexagonality and stacking sequence dependence of etching properties in Cl_2-O_2-SiC system. Mater Sci Forum 2010;645-648:771.

[20] Henry MD, Walavalkar S, Homyk A, Scherer A. Alumina etch masks for fabrication of high-aspect-ratio silicon micropillars and nanopillars. Nanotechnology 2009;20:255305.

[21] Laermer F, Schilp A. Method of anisotropic etching of silicon. United States Patent 6531068, 2003.

Figure Captions:

Figure 1. Top-view SEM images of SiC nanopillar after etching for (a-d) 360 sec, (e-h) 700 sec, and (i-l) 840 sec with different polytypes and crystallographic orientations. (a, e, i) 4H-SiC (0001) on-axis, (b, f, j) 6H-SiC (0001) on-axis, (c, g, k) 3C-SiC (001), and (d, h, l) misoriented 6H-SiC (11-20), respectively.

Figure 2. (a) Pillar height for different polytypes and orientations as a function of etching time, (b-e) the morphology of etched SiC pillars after 700 sec etching time, (b) 3C-SiC (001), (c) 4H-SiC (0001), (d) 6H-SiC (0001) and (e) 6H-SiC (11-20), respectivel**y**.